



Controlled-size embryoid body formation in concave microwell arrays

Yoon Young Choi^{a,1}, Bong Geun Chung^{b,1}, Dae Ho Lee^a, Ali Khademhosseini^{c,d}, Jong-Hoon Kim^e, Sang-Hoon Lee^{a,*}

^a Department of Biomedical Engineering, Korea University, Seoul 136-701, Republic of Korea

^b Department of Bionano Engineering, Hanyang University, Ansan 426-791, Republic of Korea

^c Center for Biomedical Engineering, Department of Medicine, Brigham and Women's Hospital, Harvard Medical School, Cambridge, MA 02139, USA

^d Harvard-MIT Division of Health Sciences and Technology, Massachusetts Institute of Technology, Cambridge, MA 02139, USA

^e Division of Biotechnology, College of Life Science and Biotechnology, Korea University, Seoul 136-705, Republic of Korea

ARTICLE INFO

Article history:

Received 9 December 2009

Accepted 18 January 2010

Available online 5 March 2010

Keywords:

Concave microwell array

Embryonic stem cell differentiation

Neurogenesis

Cardiogenesis

ABSTRACT

Embryonic stem (ES) cells hold great potential as a renewable cell source for regenerative medicine and cell-based therapy. Despite the potential of ES cells, conventional stem cell culture methods do not enable the control of the microenvironment. A number of microscale engineering approaches have been recently developed to control the extracellular microenvironment and to direct embryonic stem cell fate. Here, we used engineered concave microwell arrays to regulate the size and shape of embryoid bodies (EBs)—cell aggregate intermediates derived from ES cells. Murine ES cells were aggregated within concave microwells, and their aggregate sizes were controlled by varying the microwell widths (200, 500, and 1000 μm). Differentiation of murine ES cells into three germ layers was assessed by analyzing gene expression. We found that ES cell-derived cardiogenesis and neurogenesis were strongly regulated by the EB size, showing that larger concave microwell arrays induced more neuronal and cardiomyocyte differentiation than did smaller microwell arrays. Therefore, this engineered concave microwell array could be a potentially useful tool for controlling ES cell behavior.

© 2010 Elsevier Ltd. All rights reserved.

1. Introduction

Embryonic stem (ES) cell is a powerful cell type for studying regenerative tissues and cell-based therapies, because it can self-renew and differentiate into a variety of specific lineages [1], including cardiomyocytes [2–4] and neurons [5–9]. ES cells possess greater proliferative and differentiation potential than do adult stem cells, and can recapitulate early embryonic development. Because of these features, ES cells are of great interest to researchers in the fields of regenerative medicine and tissue replacement. One critical issue in realizing the potential of ES cells is obtaining large uniform populations of clinically relevant cell types. When allowed to grow under certain conditions, ES cells generate embryoid bodies (EBs) that form the three primary germ layers: ectoderm, mesoderm, and endoderm [10–14]. Cell-lineage specification during embryonic development is largely controlled by temporally and spatially regulated signals mediated by these three germ layers [11,15,16]. If effectively harnessed, these promising characteristics make ES cells

a potentially renewable source of cells for regenerative medicine and chronic disease treatment.

Despite the great clinical promise of ES cells, a number of technical challenges associated with culture of the ES cells stand in the way of realizing their therapeutic potential. The most significant challenge is the inability to control the microenvironment—a prerequisite for achieving homogeneous lineage-specific differentiation from heterogeneous EBs. Unfortunately, traditional hanging drop and suspension culture methods do not lend themselves to resolution of such problems. These limitations of traditional culture techniques have led to the development of various microscale technologies that possess the potential to regulate the microenvironment of ES cells [17,18].

ES cell differentiation is regulated by microenvironmental stimuli, such as cell–cell, cell–extracellular matrix, and cell–soluble factor interactions. Thus, controlling cell–microenvironment interactions is of paramount importance in directing ES cell differentiation. Non-adhesive polyethylene glycol (PEG) microwell arrays have been previously used to control the homogeneity of EB size and shape [19,20]. Recent studies on PEG microwell-mediated control of EB size have also investigated the effects on ES cell fate determination, specifically addressing cardiogenesis and vasculogenesis via

* Corresponding author. Tel.: +82 2 920 6457; fax: +82 2 920 4204.

E-mail address: dbiomed@korea.ac.kr (S.-H. Lee).

¹ These authors equally contributed to this work.

WNT signaling pathways [21]. These studies showed that WNT11 was highly expressed in larger microwells (450 μm in diameter) and ES cells cultured therein exhibited cardiogenesis. In contrast, higher expression of WNT5a in smaller microwells (150 μm in diameter) was associated with endothelial cell differentiation. In addition to PEG, polyurethane microwells containing self-assembled monolayers have been used to culture human ES cells and have been shown to allow ES cell pluripotency to be maintained [22]. In such microwells, a triethylene glycol-terminated alkanethiol self-assembled monolayer prevents cell and protein attachment. Moreover, a polydimethylsiloxane (PDMS)-based hollow sphere method has been developed for culturing EBs [23]. The resulting hollow sphere structure contains 500 μL medium, allowing for long-term (10–15 days) culture of EBs *in vitro* without medium depletion.

A surface-patterning technique (i.e. microcontact printing) has also been developed to regulate EB size-dependent ES cell differentiation and to explore the underlying stem cell biology [24–27]. For example, microcontact-printed substrates (200–800 μm in diameter) have been shown to provide control over colony size-dependent human ES cell differentiation [24]. The small interfering RNA (siRNA) and inhibition assays have shown that Smad1 activation was involved in this effect. Furthermore, micro-fabricated adhesive stencils have been used to form murine ES cell aggregates within micropatterned substrates (100–500 μm in diameter) [25]. These studies demonstrated that mesoderm and endoderm differentiation were highly induced in larger cell aggregates, whereas ectoderm differentiation was enhanced in smaller aggregates. However, previous microscale engineering

approaches still have some limitations, such as cylindrical microstructures of PEG microwells are not similar to contour of EBs and microcontact-printed substrates can only control the initial size of EBs.

We have previously developed concave and convex-based thin PDMS membrane arrays (~ 10 μm thickness) for culturing the cells [28]. Cell attachment and proliferation were affected by concave and convex surface topography. However, our previous approach analyzed the adherence and growth of single cells, not the behavior of cell aggregates. Here, we used the concave PDMS microwell array, which was similar to the contour of EBs, to culture EBs in a controlled homogeneous manner. EBs were retrieved from concave microwells after culturing for 4 days *in vitro*.

2. Materials and methods

2.1. Fabrication of concave microwell arrays

The fabrication process of concave microwell arrays is illustrated in Fig. 1. The thin PDMS membrane (~ 10 μm thickness) was spin-coated on the substrate, which contained a microscale through-hole. The membrane was deflected to form convex microstructures by applying vacuum pressure through the through-holes. A SU-8 50 prepolymer solution was uniformly applied at a thickness of 1 mm to the deformed PDMS membrane, and subsequently photo-crosslinked by exposure to UV light (365 nm wavelength). Afterward, we separated the solid SU-8 on which the convex microstructure was engraved and used this SU-8 plate as a master mold for the fabrication of concave microwell arrays as we have previously described [28]. In this study, we used PDMS concave microwell arrays with three different geometries: 200 μm width/150 μm thickness, 500 μm width/200 μm thickness, and 1000 μm width/300 μm thickness. In a parallel study, PDMS cylindrical microwells with three

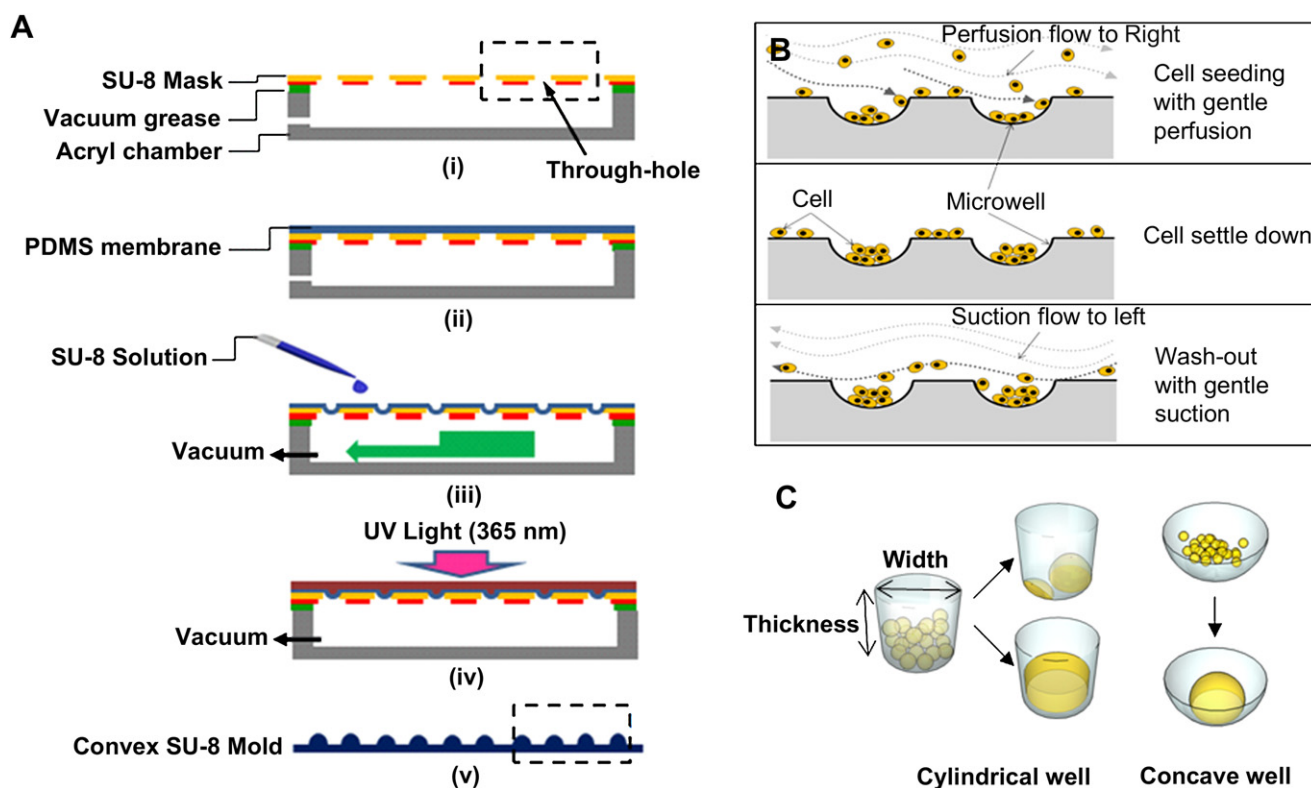


Fig. 1. (A) Schematic depiction of the process for fabricating concave microwell arrays. (i) The system consists of an acrylic chamber, vacuum grease, and a SU-8 mask surface that contains multiple through-holes. (ii) PDMS (~ 10 μm thick) is coated on the SU-8 mask surface. (iii) A SU-8 solution is layered on the PDMS membrane and negative pressure is subsequently applied through the acrylic chamber to deflect the PDMS membrane. (iv–v) The SU-8 solution is exposed to UV light (365 nm wavelength) during vacuum aspiration to create convex-shaped microstructures. The thickness of the convex-shape microstructures was controlled by the applied negative pressure. (B) Schematic process of cell seeding and docking within concave microwell structures. After gently aspirating cells that were not docked, the remaining cells docked within concave microwells were cultured as described in Materials and Methods. (C) Schematic drawing of cylindrical and concave-shaped microwell structures. The concave-shaped microwell structure is similar to the curved surface of cell aggregates.

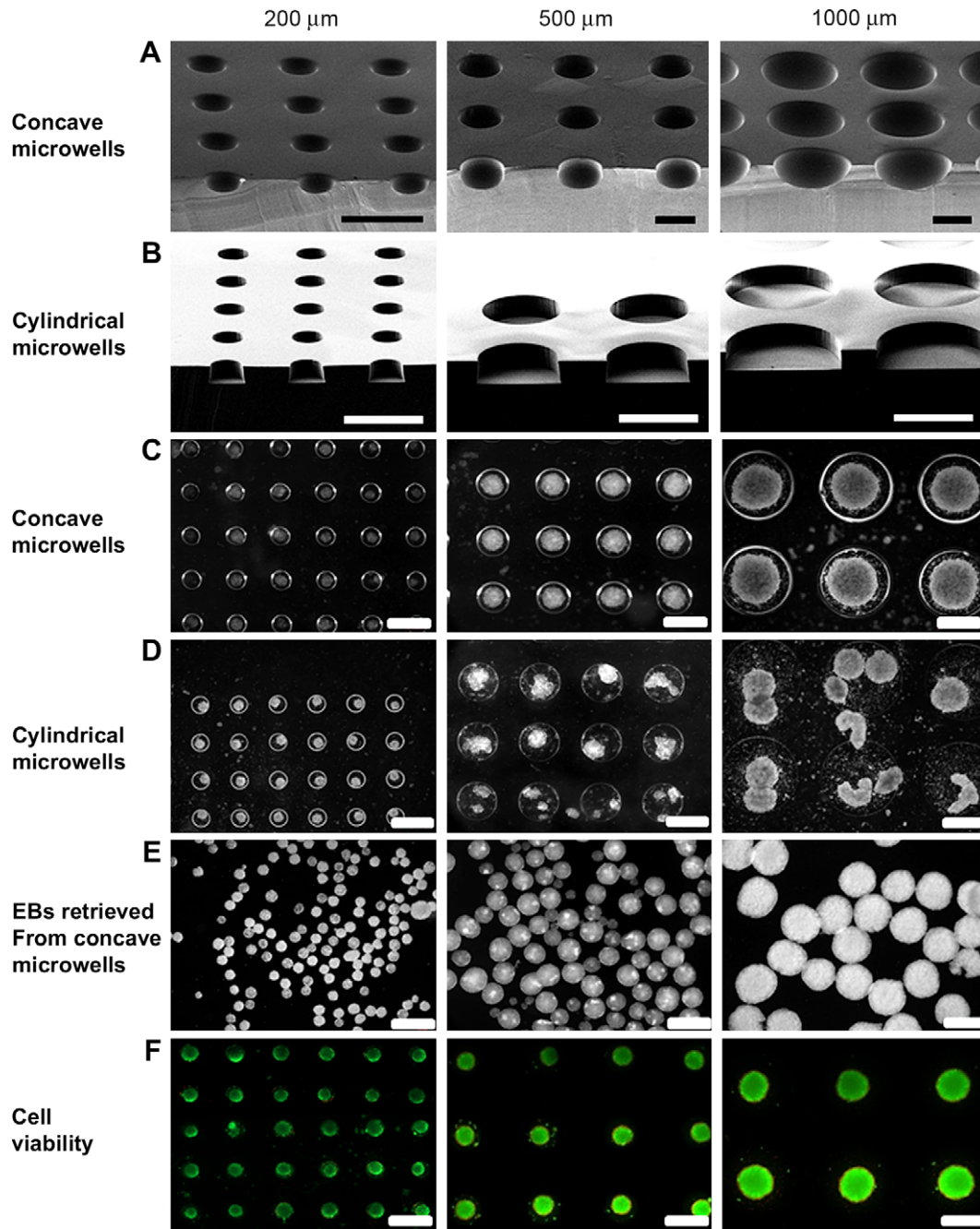


Fig. 2. EBs cultured within concave microwells with 200, 500, and 1000 μm in width. (A–B) SEM images of concave and cylindrical microwell structures with three different widths. (C) Phase contrast images of EBs formed inside concave microwells. Homogeneous-sized EBs were generated within concave microwells. (D) Phase contrast images of EBs formed within cylindrical microwells, showing heterogeneous-sized EBs. (E) EBs retrieved from concave microwells after culturing for 4 days *in vitro*. (F) Cell viability of EBs cultured for 4 days within concave microwells was analyzed by using a live/dead assay. Calcein AM stains live cells (green) and ethidium homodimer stains dead cells (red). Scale bars are 500 μm .

different geometries, such as 200 μm width/200 μm thickness, 500 μm width/300 μm thickness, and 1000 μm width/250 μm thickness, were used as a control (Fig. 2A–B).

2.2. Murine ES cell culture

The R1 ES cell line (American Type Culture Collection, Manassas, VA) used in this experiment is a sub-cell line of J1 ES cells established by Dr. Rudolph Jaenisch (Whitehead Institute for Biomedical Research, Cambridge, MA). Cells were maintained on gelatin-coated dishes and were cultured with medium consisting of 15% ES-qualified Fetal Bovine Serum (FBS, Invitrogen, CA) and 1400 Unit/ml leukemia inhibitory factor (LIF, Millipore, MA) in Dulbecco's Modified Eagle Medium (DMEM, Invitrogen, CA) knockout medium. Cells were passaged every 3 day by dissociating the cells into small colonies using 0.25%

trypsin (Invitrogen, CA) and replating on a 0.1% gelatin-coated dish at a sub-culture ratio of 1:6.

2.3. Cell seeding and EB formation within concave microwells

Murine ES cell suspension (adjusted to 1.5×10^5 cells/ml) was directly seeded on top of concave microwells without using the medium flow, allowing the cells to become trapped within concave microwells (Fig. 1B). Most cells were evenly docked within concave microwells. After 30 min of the cell seeding, the flow of culture medium was gently applied to remove cells that did not dock within microwells. A schematic depiction of cell aggregation in the concave microwell is illustrated in Fig. 1C, which shows the initial aggregation of cells at the center of concave microwells due to the effects of gravity and the subsequent formation of hemispherical EBs with uniform size and shape (Fig. 2C). In contrast, the flat surface of

Table 1

The number of EBs formed within 200, 500, and 1000 μm wide concave microwells. ES cells were cultured for 1 day within concave microwells. Single EBs were formed within smaller concave microwells (200 μm in width), whereas multiple EBs were generated within larger concave microwells (1000 μm in width).

Mold diameter	Multiple formation of EBs	
200 μm	Single	97.79%
	Double	2.21%
	Triple	0%
500 μm	Single	84.48%
	Double	11.20%
	Triple	4.31%
1000 μm	Single	56.25%
	Double	18.75%
	Triple	25%

PDMS-based cylindrical microwells makes it difficult for the cells to aggregate as a single EB, resulting in the formation of non-uniformly shaped EBs (e.g., dumbbell or island shaped; Fig. 2D).

2.4. Live and dead assay

The viability of ES cells cultured within concave microwells was analyzed by using a live/dead assay (Invitrogen, CA) (Fig. 2F). Briefly, 5 mL of phosphate-buffered saline (PBS) containing 2 μL of calcein AM solution and 10 μL of ethidium homodimer-1 solution was added to concave microwells and was then incubated at 37 $^{\circ}\text{C}$ in a 5% CO_2 incubator for 40 min. The stained ES cells were analyzed by using an inverted fluorescence microscope.

2.5. Three germ layer differentiation of EBs and gene analysis

Murine ES cells were cultured within concave microwells for 4 and 8 days *in vitro*. The EBs formed within each of the three different-sized concave microwells were gently retrieved and subsequently resuspended in Knockout-DMEM containing 15% FBS, non-essential amino acids, 2 mM L-Glutamine, β -mercaptoethanol (Invitrogen, CA), and penicillin-streptomycin. The cells were also digested in TRIzol Reagent (Invitrogen, CA), followed by chloroform extraction and precipitation with isopropyl alcohol. cDNA was generated from purified RNA using reverse transcriptase (TAKARA, Japan) as based on the manufacturer's instructions.

2.6. Immunostaining analysis

Murine ES cell-derived neural progenitor cells grown within concave microwells were analyzed immunocytochemically to confirm the spatial distribution of neuroectodermal cells. After culturing for 4 days within concave microwells, cells were retrieved and were cultured with neural differentiation medium on tissue culture dishes for an additional 6 days. The cells cultured for 10 days were fixed for 20 min with 4% formaldehyde at 4 $^{\circ}\text{C}$. Cells were permeabilized by using 0.1% Triton-X100 in 0.1% PBS for 20 min at room temperature, blocked with 3% BSA in PBS for 30 min, and were then incubated with primary antibody overnight at 4 $^{\circ}\text{C}$. Primary antibodies (Stemcell Technologies, Canada) against the following proteins were used to characterize various cell types: neurofilament (1:1000) nestin (1:100), and glial fibrillary acidic protein (GFAP; 1:100). After incubating overnight, each microwell was washed with PBST (0.05% Tween in PBS) for 5 min. Secondary antibodies (1:1000 dilutions, Invitrogen, CA) were applied for 1.5 h at room temperature. Each concave microwell was washed with PBST, and fluorescence images were acquired by using a fluorescence microscope (AxioVision 4, Germany) after counterstaining with 4,6-diamidino-2-phenylindole dihydrochloride (DAPI, Invitrogen, CA).

2.7. Culture conditions for ES cell-derived cardiac differentiation

EBs within concave microwells were cultured by using ES cell culture medium for 4 days. After 4 days, EBs within concave microwells were cultured with cardiac differentiation culture medium, such as MEM- α (Gibco), 15% FBS, 1% penicillin/streptomycin. We measured the beating of EBs cultured within concave microwells for 10 days.

2.8. Culture conditions for ES cell-derived neuronal differentiation

EBs cultured within concave microwells for 4 days *in vitro* were retrieved and replated onto tissue culture dishes. Neuronal differentiation was induced by culturing EBs with insulin/transferrin/selenium/fibronectin (ITSFn) medium (Invitrogen, CA). On day 10, cells exhibiting the morphology of neuroepithelial cells were observed. To obtain a large number of neural progenitor cells with high purity, we dissociated differentiated cells from EBs with 0.05% trypsin (Invitrogen,

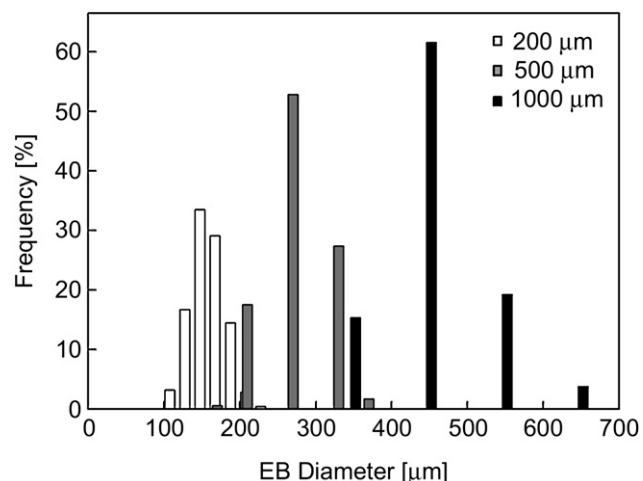


Fig. 3. Quantitative analysis of EB diameter distribution. EBs retrieved from concave microwells after culturing for 4 days *in vitro* were more homogeneous in size and their sizes were significantly regulated by microwell widths (200, 500, and 1000 μm).

CA), resuspended them in N2 medium (Invitrogen, CA) containing human basic fibroblast growth factor (bFGF, 20 ng/mL), and replated them at a density of 2×10^6 cells/cm² on plates coated with poly-L-ornithine (PLO; 50 $\mu\text{g}/\text{mL}$, Sigma, MO) and laminin (5 $\mu\text{g}/\text{mL}$). After culturing for 14 days, ES cells were cultured with N2 medium without human bFGF for an additional 7 days to enhance neuronal differentiation.

3. Results and discussion

3.1. Concave microwell arrays to culture ES cells

To generate concave microwells, we employed a simple three-dimensional (3D), curved-microstructure fabrication technique (Fig. 1) as previously described [28]. Briefly, to create the concave-shape microwell, we applied negative pressure through an acrylic chamber. The SU-8 prepolymer on the PDMS membrane was deflected to form convex SU-8 microstructures. Thus, the concave PDMS microwell was fabricated from the convex mold microstructure. To culture ES cells within concave microstructures, we seeded the cells into concave microwells, allowing the cells to dock within the microwells. One major feature of this system is that the resulting EB shape is similar to the concave microwell array structure in which they are grown, in contrast to previously reported non-adhesive PEG microwells with cylindrical shapes [19–21]. Scanning electron microscopy (SEM) images showed concave microwell arrays with 200, 500, and 1000 μm widths (Fig. 2A).

Although previous studies have been used by conventional soft lithographic techniques [18,29], such methods have the inability to control the 3D microstructures. A few studies have recently reported the techniques for fabricating smooth, curved microstructures; these include ice droplet-based microcavity formation [30], deep reactive ion etching (DRIE) [31], cylindrical microchannel formation using a water mold [32], and electroplating [33]. The concave PDMS-based microwell system is an attractive method, because it can be used to control the formation of homogeneous-sized EBs, which are important factor to control specific lineage differentiation [34,35]. Furthermore, this system can be used to fabricate larger microwell structures (>500 μm in width), because the microwell size is only controlled by the applied negative pressure and the concave microstructure is largely dependent on the stretchable property of PDMS (shear elastic modulus, $G \approx 250$ kPa).

3.2. EBs cultured in concave microwells

EBs were harvested after culturing for 4 days within concave microwells of three different widths (200, 500, and 1000 μm). ES cells cultured in concave microwells were physically constrained and formed EBs that were homogeneous in size (Fig. 2E). Cell viability analysis demonstrated that cells cultured for 4 days within concave microwell arrays remained viable regardless of the microwell widths (Fig. 2F). Thus, the concave microwell array could be a potentially useful tool for culturing ES cells *in vitro*.

Multiple formation of EBs cultured within concave microwells for 1 day *in vitro* was analyzed (Table 1). It indicated that cell aggregates cultured within concave microwells showed the single EB formation. The probability of forming a single EB was much higher in smaller (200 μm in width) concave microwells (97.79%) than in larger (1000 μm in width) concave microwells (56.25%). Multiple EBs were more easily generated within larger concave microwells because of the larger surface areas of such microwells. Furthermore, cells cultured within concave microwells generated single EBs more readily than did cells in cylindrically shaped microwells, because the shape of the concave microwell is similar to that of the curved EB surface (Fig. 2C–D). In the cylindrical PDMS microwell, smaller EBs were generated at the edge of larger microwells (Fig. 2D), probably because of the hydrophobic and cell-adherent properties of the PDMS substrate. Previous studies have demonstrated that PEG microwells enable the control of homogeneity of EB size and shape, because hydrophilic PEG has cell and protein-repellent properties [19–21]. However, hydrophobic PDMS does not have the strong cell-repellent properties of PEG. Thus, larger cylindrically shaped PDMS microwells generated multiple and smaller EBs.

EBs were retrieved from concave microwells and the distribution of their diameters was analyzed (Fig. 3). EB concentration means the size distribution of EBs retrieved from concave microwells after culturing for 4 days *in vitro*. An EB concentration analysis

showed that smaller concave microwells facilitated the formation of homogeneous-sized cell aggregates. We confirmed that the size of EBs cultured within smaller concave microwells was similar to the original size of the microwells. In contrast, the size of EBs cultured in larger concave microwells was approximately half of the original microwell size.

3.3. Three germ layer differentiation

We analyzed three germ layer differentiation of EBs cultured within concave microwells by evaluating the expression of gene markers on day 4 and 8 (Fig. 4). We found no evidence for expression of the endodermal differentiation marker, AFP, in any of the three sizes of microwells on day 4. On day 8, however, AFP was highly expressed in EBs grown in the larger microwells (500 and 1000 μm in width), but remained undetectable in EBs grown in small microwells (200 μm in width), indicating that endodermal differentiation was enhanced in larger EBs at day 8. An analysis of the time-dependent expression of nestin, a marker for ectoderm differentiation, showed that although nestin expression was higher in smaller EBs at day 4, the expression of ectoderm in larger EBs surpassed that in smaller EBs at day 8. In contrast, we found no significant size-dependent difference in mesoderm differentiation as based on expression of the BMP4 (bone morphogenetic protein 4) marker. This analysis also showed that cells were differentiated into mesoderm at an earlier stage as compared to endoderm and ectoderm differentiation. Therefore, gene expression data indicated that three germ layer differentiation was affected by homogeneous-sized EBs.

3.4. Neural differentiation

We analyzed EB size-dependent ES cell differentiation into neuronal cells. After culturing within concave microwells for 4 days *in vitro*, EBs were harvested from the concave microwells,

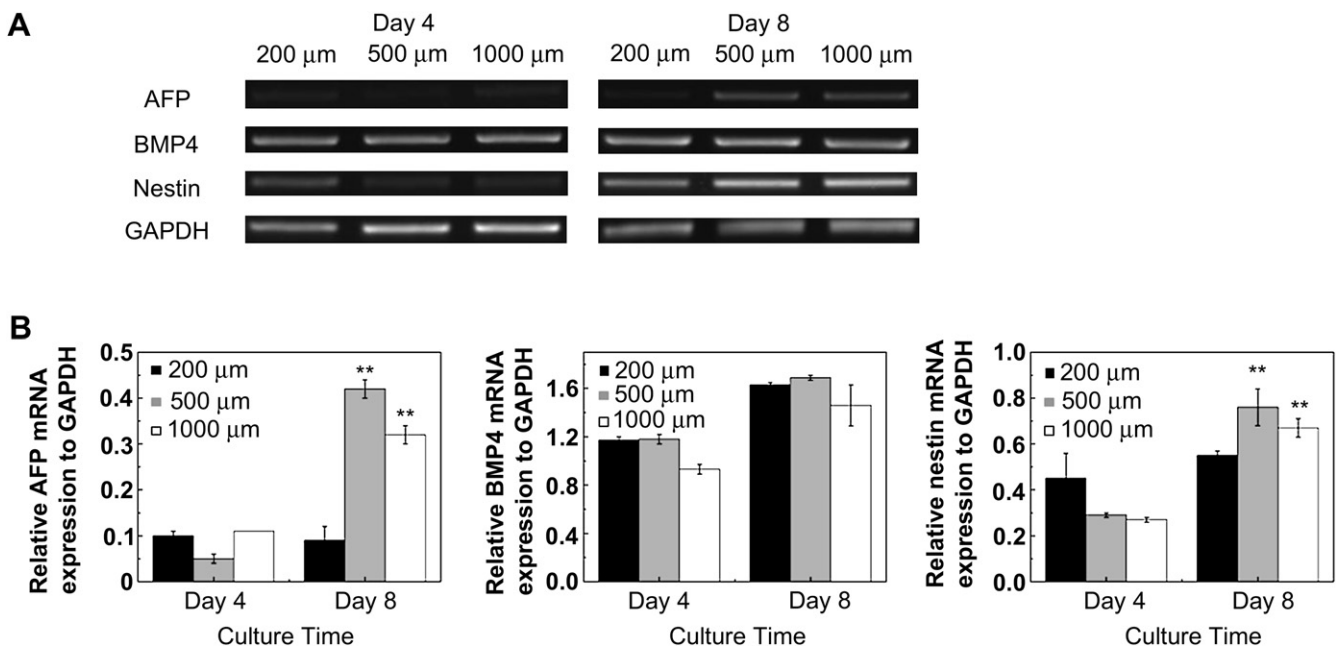


Fig. 4. Time-course of expression of markers for the three germ layers in EBs. (A) A representative gel showing expression of mRNA for three germ layer markers in ES cells cultured within concave microwells for 4 and 8 days *in vitro*. (B) The quantification of relative gene expression of AFP (endoderm), BMP4 (mesoderm), and nestin (ectoderm) on day 4 and 8. The gene expression results show a greater degree of endoderm and ectoderm differentiation in larger concave microwells (500 and 1000 μm in width). Error bars are standard deviation and ** indicates $p < 0.01$ as compared to 200 μm EBs ($n = 3$; Student's t -test).

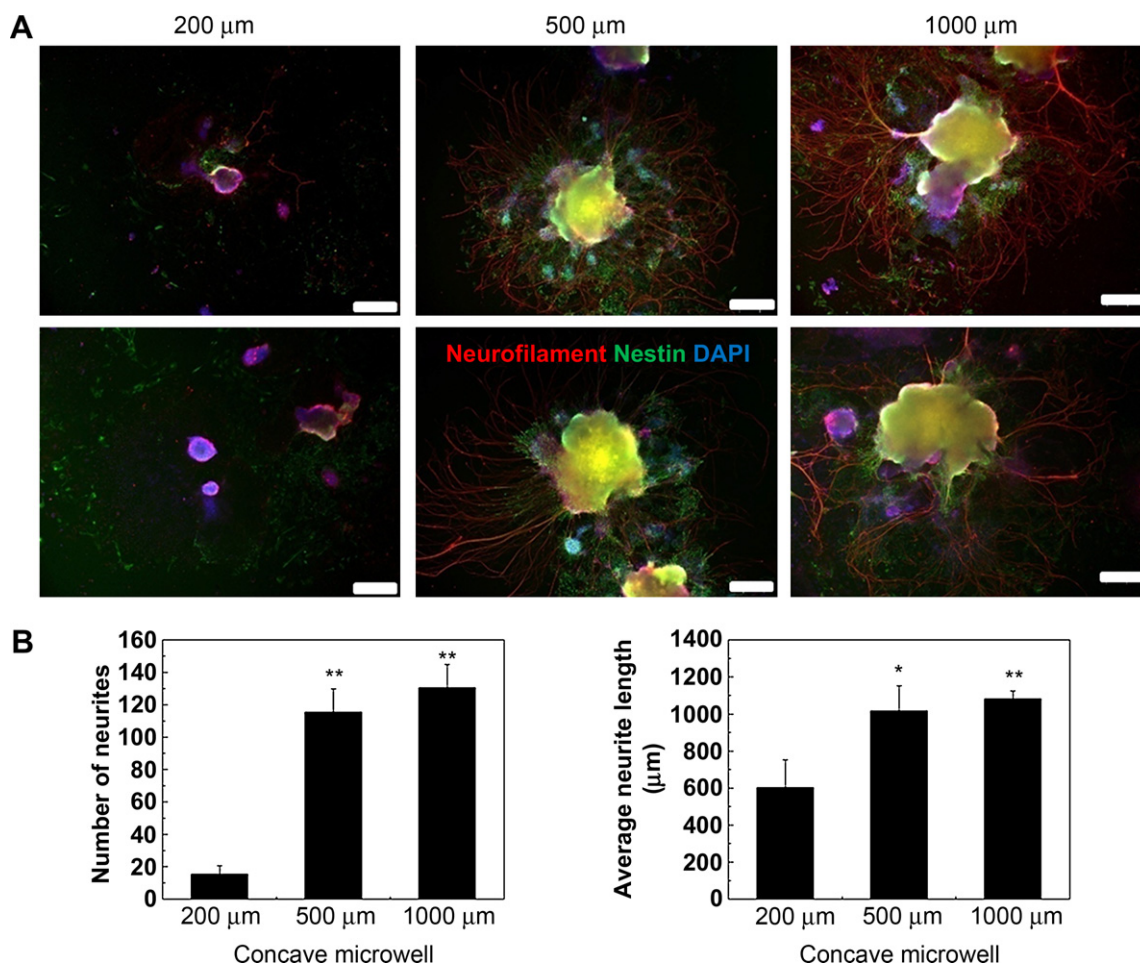


Fig. 5. (A) Fluorescent images showing ES cell-derived neuronal differentiation. ES cells cultured within concave microwells for 4 days were retrieved and were cultured with neural differentiation medium on tissue culture dishes for an additional 6 days. After culturing for 10 days, the cells were stained for neurofilaments (red) and nestin (green) to identify neurites and neural precursor cells, respectively; nuclei were stained with DAPI (blue). (B) Quantitative analysis of neurite numbers and lengths from EBs retrieved from concave microwells, showing that larger EBs had a greater number of neurites and longer neurite outgrowth than smaller EBs. Error bars are standard deviation; * and ** indicate $p < 0.05$ and $p < 0.01$ as compared to 200 μm EBs ($n = 3$; Student's t -test). Scale bars are 500 μm .

transferred to tissue culture dishes, and cultured in differentiation medium containing fibronectin (20 $\mu\text{g}/\text{mL}$) for an additional 6 days, resulting in neuroepithelial differentiation (Fig. 5). The EBs were fixed and were immunostained with the neurofilament, nestin, and counterstained with DAPI. The results indicated that EB sprouting was more prominent in EBs retrieved from larger concave microwells than from smaller microwells. The EB sprouting represented neurite outgrowth that was confirmed by positive staining for neurofilaments (Fig. 5A). Larger EBs retrieved from concave microwells (500 and 1000 μm in width) were similar to neurospheres, which showed the potential to generate neurite outgrowth. In contrast, we found only a few neurite outgrowth in EBs retrieved from smaller concave microwells (200 μm in width).

To further quantify neurite outgrowth activities, we analyzed neurite numbers and average neurite lengths by using an Image J program (Fig. 5B). These quantitative analyses showed that the average number of neurites in EBs grown in concave microwells with 200, 500, and 1000 μm in width was 15, 115, and 130, respectively. We found significant differences of neurite numbers between smaller EBs (200 μm microwell in width) and larger EBs (500 and 1000 μm microwell in width). The average lengths of neurites were 600, 1010, and 1080 μm in EBs grown in microwells with 200, 500, and 1000 μm in width. The larger EBs also

contained a greater number of neuronal cells, indicating that larger concave microwells (500 and 1000 μm in width) induced more EB size-dependent neural differentiation. In a parallel study, we analyzed neuronal differentiation of ES cells in EBs cultured on Petri dishes (Supplementary Fig. 1). We found that individual ES cells were differentiated into morphologically identifiable glial cells, such as star-like astrocytes, that were confirmed to be positive for the glial cell marker, glial fibrillary acidic protein (GFAP). Furthermore, neurofilament-positive neurite outgrowth was observed in EBs grown on Petri dishes and neurites were interconnected between each EB. Thus, the neurite outgrowth behavior of EBs retrieved from concave microwells was similar to that of control EBs cultured on Petri dishes. We also analyzed EBs from the three different-sized microwells for tyrosine hydroxylase (TH) expression (Supplementary Fig. 2), indicating dopaminergic neuronal differentiation. To induce dopaminergic neuronal differentiation, we isolated ES cells from EBs by trypsinization and transferred ES cell suspensions to poly-L-ornithine- and laminin-treated culture dishes, as described in Materials and Methods. We found the high purity of dopaminergic neurons in ES cells derived from EBs cultured in all three concave microwells (200, 500, and 1000 μm in width). It was revealed that ES cell-derived dopaminergic neuronal differentiation was not affected by homogeneous EB sizes.

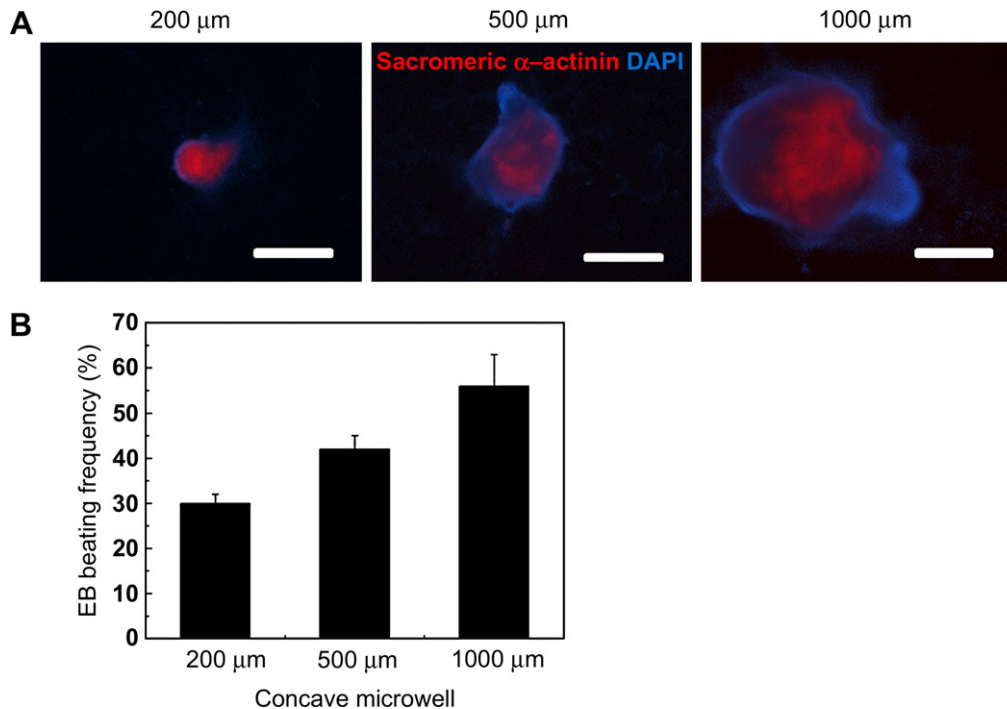


Fig. 6. ES cell-derived cardiac differentiation. (A) Fluorescent images of immunostained EBs cultured for 10 days within concave microwells showing cardiac differentiation. The cells were immunostained by sarcomeric α -actinin (red) and DAPI (blue). (B) The beating frequency of EBs cultured within concave microwells. EB beating frequency refers to the number of concave microwells containing beating EBs divided by the total number of concave microwells. Error bars are standard deviation and Scale bars are 500 μ m.

3.5. Cardiac differentiation

To analyze EB size-dependent cardiogenesis, the cells were immunostained by the sarcomeric α -actinin (Fig. 6A). We characterized cardiac function by measuring beating frequency (Fig. 6B). The EB beating frequency refers to the number of concave microwells containing beating EBs divided by the total number of concave microwells. A quantitative analysis of EB beating demonstrated that the frequency of spontaneous beating was strongly dependent on the EB size. We found a higher frequency of beating (56%) in larger EBs (1000 μ m microwell in width) than in smaller EBs (200 μ m microwell in width), where the beating frequency was approximately 30%. Furthermore, immunostaining images indicated that cells cultured within microwells with 1000 μ m in width showed relatively high expression of sarcomeric α -actinin as compared to microwells with 200 μ m and 500 μ m in width. It is probably due to the higher total cell number of larger EBs cultured within microwells with 1000 μ m in width. This EB size-dependent cardiac differentiation, which is consistent with the recent report [21], may reflect the fact that larger cell aggregates can significantly affect cardiac function and beating frequency.

4. Conclusions

We developed a PDMS-based concave microwell system that enables the control of homogeneous EB sizes and demonstrated that EB size is a determining factor in ES cell differentiation. Specifically, we found that cardiac and neuronal differentiation was regulated by the size of cell aggregates. EBs cultured within larger concave microwells showed higher beating frequency and higher neurite outgrowth activity as compared to smaller microwells. Given these properties of EB size-dependent differentiation, concave microwell arrays that enable the production of homogeneous-sized cell aggregates could be a potentially useful tool for directing ES cell fate.

Acknowledgements

This paper is supported by the Korea Science and Engineer Foundation (KOSEF) (grant no. ROA-2007-000-20086-0) and this work was also supported by the Korea Research Foundation Grant funded by the Korean Government (MEST) (KRF-2008-220-D00133).

Appendix. Supplementary material

Supplementary Fig. 1 Fluorescent images showing ES cell-derived neuronal differentiation. ES cells were cultured for 21 days on a Petri dish as a control. ES cells differentiated into star-like astrocytes, which were confirmed by GFAP staining (green). Scale bars are 200 μ m.

Supplementary Fig. 2 Differentiation of TH-positive dopaminergic neurons from ES cells cultured within concave microwells. TH, nestin, and DAPI indicate dopaminergic neurons (green), neural precursor cells (red), and cell nuclei (blue), respectively. EBs cultured within different-sized concave microwells for 4 days were transferred to tissue culture dishes for an additional 17 days to enhance dopaminergic neuronal differentiation. Scale bars are 100 μ m.

Note: Supplementary material associated with this article can be found in the online version, at [doi:10.1016/j.biomaterials.2010.01.115](https://doi.org/10.1016/j.biomaterials.2010.01.115).

Appendix

Figures with essential color discrimination. Figs. 1, 2, 5 and 6 in this article are difficult to interpret in black and white. The full color images can be found in the online version, at [doi:10.1016/j.biomaterials.2010.01.115](https://doi.org/10.1016/j.biomaterials.2010.01.115).

References

- [1] Bhattacharya B, Puri S, Puri RK. A review of gene expression profiling of human embryonic stem cell lines and their differentiated progeny. *Curr Stem Cell Res Ther* 2009;4(2):98–106.

- [2] Mummery C, Ward-van Oostwaard D, Doevendans P, Spijker R, van den Brink S, Hassink R, et al. Differentiation of human embryonic stem cells to cardiomyocytes: role of coculture with visceral endoderm-like cells. *Circulation* 2003;107(21):2733–40.
- [3] Kehat I, Gepstein A, Spira A, Itskovitz-Eldor J, Gepstein L. High-resolution electrophysiological assessment of human embryonic stem cell-derived cardiomyocytes: a novel in vitro model for the study of conduction. *Circ Res* 2002;91(8):659–61.
- [4] Kehat I, Kenyagin-Karsenti D, Snir M, Segev H, Amit M, Gepstein A, et al. Human embryonic stem cells can differentiate into myocytes with structural and functional properties of cardiomyocytes. *J Clin Invest* 2001;108(3):407–14.
- [5] Kim JH, Auerbach JM, Rodriguez-Gomez JA, Velasco I, Gavin D, Lumelsky N, et al. Dopamine neurons derived from embryonic stem cells function in an animal model of Parkinson's disease. *Nature* 2002;418(6893):50–6.
- [6] Bjorklund LM, Sanchez-Pernaute R, Chung S, Andersson T, Chen IY, McNaught KS, et al. Embryonic stem cells develop into functional dopaminergic neurons after transplantation in a Parkinson rat model. *Proc Natl Acad Sci U S A* 2002;99(4):2344–9.
- [7] Zhang SC, Wernig M, Duncan ID, Brustle O, Thomson JA. In vitro differentiation of transplantable neural precursors from human embryonic stem cells. *Nat Biotechnol* 2001;19(12):1129–33.
- [8] Schuldiner M, Eiges R, Eden A, Yanuka O, Itskovitz-Eldor J, Goldstein RS, et al. Induced neuronal differentiation of human embryonic stem cells. *Brain Res* 2001;913(2):201–5.
- [9] Reubinoff BE, Itsykson P, Turetsky T, Pera MF, Reinhartz E, Itzik A, et al. Neural progenitors from human embryonic stem cells. *Nat Biotechnol* 2001;19(12):1134–40.
- [10] Wobus AM, Boheler KR. Embryonic stem cells: prospects for developmental biology and cell therapy. *Physiol Rev* 2005;85(2):635–78.
- [11] Thomson JA, Itskovitz-Eldor J, Shapiro SS, Waknitz MA, Swiergiel JJ, Marshall VS, et al. Embryonic stem cell lines derived from human blastocysts. *Science* 1998;282(5391):1145–7.
- [12] Ling V, Neben S. In vitro differentiation of embryonic stem cells: immunophenotypic analysis of cultured embryoid bodies. *J Cell Physiol* 1997;171(1):104–15.
- [13] Itskovitz-Eldor J, Schuldiner M, Karsenti D, Eden A, Yanuka O, Amit M, et al. Differentiation of human embryonic stem cells into embryoid bodies compromising the three embryonic germ layers. *Mol Med* 2000;6(2):88–95.
- [14] Pezeron G, Mourrain P, Courty S, Ghislain J, Becker TS, Rosa FM, et al. Live analysis of endodermal layer formation identifies random walk as a novel gastrulation movement. *Curr Biol* 2008;18(4):276–81.
- [15] Zandstra PW, Nagy A. Stem cell bioengineering. *Annu Rev Biomed Eng* 2001;3:275–305.
- [16] Winston R. Embryonic stem cell research-The case for. *Nat Med* 2001;7(4):396–7.
- [17] Khademhosseini A, Langer R, Borenstein J, Vacanti JP. Microscale technologies for tissue engineering and biology. *Proc Natl Acad Sci U S A* 2006;103(8):2480–7.
- [18] Whitesides GM, Ostuni E, Takayama S, Jiang X, Ingber DE. Soft lithography in biology and biochemistry. *Annu Rev Biomed Eng* 2001;3:335–73.
- [19] Karp JM, Yeh J, Eng G, Fukuda J, Blumling J, Suh KY, et al. Controlling size, shape and homogeneity of embryoid bodies using poly(ethylene glycol) microwells. *Lab Chip* 2007;7(6):786–94.
- [20] Moeller HC, Mian MK, Shrivastava S, Chung BG, Khademhosseini A. A microwell array system for stem cell culture. *Biomaterials* 2008;29(6):752–63.
- [21] Hwang YS, Chung BG, Ortmann D, Hattori N, Moeller HC, Khademhosseini A. Microwell-mediated control of embryoid body size regulates embryonic stem cell fate via differential expression of WNT5a and WNT11. *Proc Natl Acad Sci U S A* 2009;106(40):16978–83.
- [22] Mohr JC, de Pablo JJ, Palecek SP. 3-D microwell culture of human embryonic stem cells. *Biomaterials* 2006;27(36):6032–42.
- [23] Lee WG, Ortmann D, Hancock MJ, Bae H, Khademhosseini A. A hollow sphere soft lithography approach for long-term hanging drop methods. *Tissue Eng Part C Methods*, in press, doi:10.1089/ten.tec.2009.0248.
- [24] Peerani R, Rao BM, Bauwens C, Yin T, Wood GA, Nagy A, et al. Niche-mediated control of human embryonic stem cell self-renewal and differentiation. *EMBO J* 2007;26(22):4744–55.
- [25] Park J, Cho CH, Parashurama N, Li Y, Berthiaume F, Toner M, et al. Microfabrication-based modulation of embryonic stem cell differentiation. *Lab Chip* 2007;7(8):1018–28.
- [26] Lee LH, Peerani R, Ungrin M, Joshi C, Kumacheva E, Zandstra P. Micropatterning of human embryonic stem cells dissects the mesoderm and endoderm lineages. *Stem Cell Res* 2009;2(2):155–62.
- [27] Peerani R, Onishi K, Mahdavi A, Kumacheva E, Zandstra PW. Manipulation of signaling thresholds in “engineered stem cell niches” identifies design criteria for pluripotent stem cell screens. *PLoS One* 2009;4(7):e6438.
- [28] Park JY, Lee DH, Lee EJ, Lee SH. Study of cellular behaviors on concave and convex microstructures fabricated from elastic PDMS membranes. *Lab Chip* 2009;9(14):2043–9.
- [29] Xia YN, Whitesides GM. Soft lithography. *Annu Rev Mater Sci* 1998;28:153–84.
- [30] Park JY, Hwang CM, Lee SH. Ice-lithographic fabrication of concave microwells and a microfluidic network. *Biomed Microdevices* 2009;11:129–33.
- [31] Giang UB, Lee D, King MR, DeLouise LA. Microfabrication of cavities in polydimethylsiloxane using DRIE silicon molds. *Lab Chip* 2007;7(12):1660–2.
- [32] Chao SH, Carlson R, Meldrum DR. Rapid fabrication of microchannels using microscale plasma activated templating (mu PLAT) generated water molds. *Lab Chip* 2007;7(5):641–3.
- [33] Yi Y, Kang JH, Park JK. Moldless electroplating for cylindrical microchannel fabrication. *Electrochem Comm* 2005;7(9):913–7.
- [34] Dang SM, Kyba M, Perlingeiro R, Daley GQ, Zandstra PW. Efficiency of embryoid body formation and hematopoietic development from embryonic stem cells in different culture systems. *Biotechnol Bioeng* 2002;78(4):442–53.
- [35] Torisawa YS, Chueh BH, Huh D, Ramamurthy P, Roth TM, Barald KF, et al. Efficient formation of uniform-sized embryoid bodies using a compartmentalized microchannel device. *Lab Chip* 2007;7(6):770–6.